ELSEVIER
Wear 253 (2002) 618–625
WEAR
www.elsevier.com/locate/wear

Creep and wear behaviour of ethylene–butene copolymers reinforced by ultra-high molecular weight polyethylene fibres

O. Jacobs [a,*], M. Kazanci [b], D. Cohn [b], G. Marom [b]

[a] Department of Mechanical Engineering, Fachhochschule Lübeck—University of Applied Science, Stephensonstr. 3, 23562 Lübeck, Germany
[b] Casali Institute of Applied Chemistry, The Hebrew University of Jerusalem, 91904 Jerusalem, Israel

Received 12 October 2001; received in revised form 4 April 2002; accepted 30 April 2002

Abstract

Filament wound flat strips of polyethylene–butene copolymers (PE) reinforced by continuous fibres of ultra-high molecular weight polyethylene (UHMWPE) were tested in a ball-on-prism tribometer against steel balls. The winding angle ($\tau = 35$ and 50°) and the branching ratio (flexibility) of the matrix polymer were varied. The static penetration of the ball into the sample material (creep), the running-in wear and the steady-state wear were measured.

The creep resistance of the neat matrices decreased significantly with increasing branching of the copolymer. All fibre reinforced versions had almost the same creep resistance as the stiffest matrix polymer. The running-in wear was governed by the peeling-off of a thin matrix layer which happened rather fast. During the steady-state phase, the wear was controlled by the wear resistance of the fibres. All composites revealed the same wear rate. Strong fibrillation of the composites was observed.

Keywords: Ethylene–butene copolymers; Ultra-high molecular weight polyethylene; Fibre; Ultra-high molecular weight polyethylene fibres; Creep; Sliding wear

1. Introduction

Ultra-high molecular weight polyethylene (UHMWPE) which exhibits very low friction coefficient, high wear resistance and high impact strength is widely used in biomedical applications [1,2]. The primary application of the UHMWPE as a biomedical implant has been in acetabular cup components in total hip replacement [3]. The major cause of failure for these prosthesis is due to the cellular events induced by the PE wear debris coming from the bearing surfaces [4]. This is the same mechanism that leads the failure of ligament and tendon prostheses [5].

In the past, a great deal of work has been done on understanding the factors that affect the wear of UHMWPE and on structural modifications and surface treatments to reduce its wear [6,7]. Since UHMWPE is a viscoelastic material, its performance is affected by inherent weaknesses, such as high creep compared to the metal stem and bone. Unfortunately, most of the commercial ligament prostheses undergo mechanical failure due to their weak resistance to bending and friction [8]. To extend the lifetime of artificial joints, it is necessary to decrease the wear rate, which in turn reduces the number and volume of generated debris. Reinforcing the polymers with fibres is known to improve not only their mechanical properties, but also their tribological properties [9].

The objective of this work is to study the creep and wear behaviour of filament wound, flat strip composites of polyethylene fibre reinforced polyolefins intended for use as synthetic ligament and tendon implants. The versatility of the new product is demonstrated by involving different polyolefin compositions based on polyethylene–butene copolymers and two different winding angles. In three previous papers, the effects of these parameters on the elastic, viscoelastic and fatigue behaviour of the composite materials were investigated [10,11], as well as the effects of processing conditions, and gas sterilisation on the surface oxidation and cell attachment [12].

2. Experimental details

2.1. Sample preparation

For the matrix, three different polyethylene–butene copolymers (named 4011, 4015 and 4041) of the Exact

* Corresponding author. Tel.: +49-451-300-5323; fax: +49-451-300-5302.
E-mail address: jacobs@fh-luebeck.de (O. Jacobs).

0043-1648/02/$ – see front matter © 2002 Elsevier Science B.V. All rights reserved.
PII: S0043-1648(02)00110-2

Table 1
Properties of the matrix materials

Matrix	Branching (per 1000 main chain C atoms)	Yield stress (MPa)	Strain (%)	Modulus (MPa)	Crystallinity (%)
Exact 4041	66	1.5	27	22	10
Exact 4011	50	2.1	23	30	13
Exact 4015	42	2.8	22	42	17

family from ExxonMobile were used. The mechanical properties and the level of branching are given in Table 1.

Composite materials were produced by embedding Spectra 1000 UHMWPE fibres (Allied Signal) in the copolymer matrices.

The copolymers were supplied in pellet form, from which 0.25 mm thick sheets were moulded by pressing at 100 °C under a pressure of 6.25 MPa (Carver Laboratory Press), followed by removing them from the press and cooling in an ice-water bath. Filament winding was performed using a bench winder (Burlington Instruments Co., Vermont) as described in [13]. A flat mandrel (10 mm wide, 0.5 mm thick and 135 mm long) was wrapped by a matrix film onto which the fibre was wound at a designated angle, and then wrapped by a second matrix film to produce a preform. The resulting preform was carefully removed from the mandrel and pressed at 100 °C under 10 MPa for 30 min, followed by ice-water cooling. Specimens of two winding angles (35 and 50°) were produced with a fibre weight fraction of about 0.65. Fig. 1 shows a photograph of a specimen produced in this way. Additional experimental details and pictures of the filament wound products can be found in [10,11].

From the flat strip specimens, 10 mm × 10 mm × 1.5 mm samples were cut. The composites were designated by a suffix which specified the winding angle (e.g. 4011–35 versus 4011–50).

2.2. Testing procedures

2.2.1. Test rig

For an initial screening, the wear tests were performed in a simple standard ball-on-prism tribometer under dry condition which is described in detail in [14,15]. Here the basic features are summarised.

Fig. 2a shows a schema of the set-up. A metallic prism with an opening angle of 90° containing the specimens was pressed against a steel bearing ball ($R_a = 0.05\ \mu$m). Dead weights were attached to the lever so that the specimens were

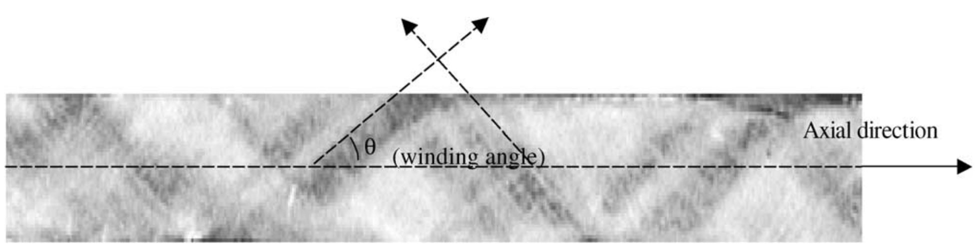

Fig. 1. Photograph of a filament wound composite strip.

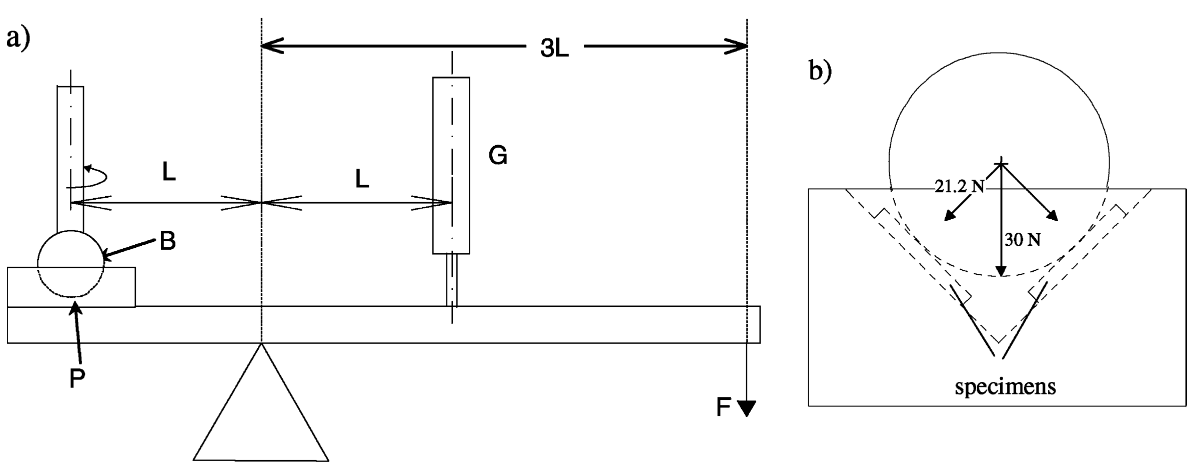

Fig. 2. Schematic of the wear testing apparatus used for the wear and creep tests (a) P: specimen holder (prism), B: steel ball rotating around the vertical axis, G: inductive displacement transducer, F: dead weight (10 N) and (b) magnified front view of the specimen holder with inserted specimens loaded by the steel ball.

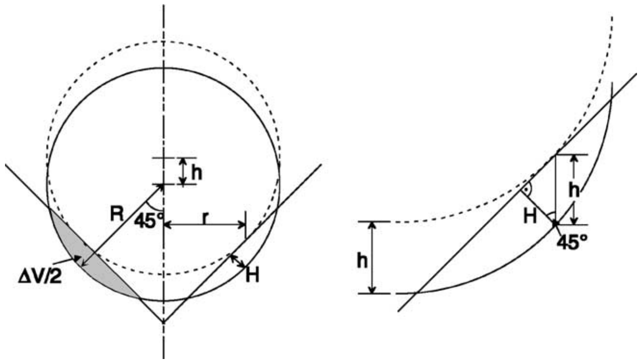

Fig. 3. Relation between vertical motion, *h*, of the lever and penetration of the steel ball into the specimen surface, *H*.

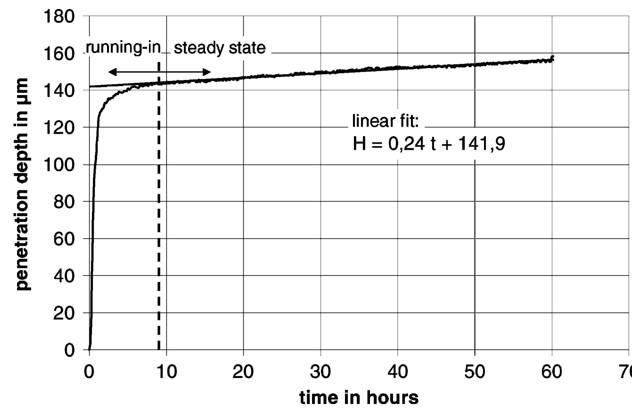

Fig. 4. Wear curve for UHMWPE fibre reinforced 4015 (low branching).

pressed against the balls with a force of 30 N. The normal load acting on each specimen was $F_N = (30/2)\sqrt{2}\,N = 21.2\,N$ (Fig. 2b).

For the first screening tests, simple bearing balls of hardened 100Cr6 steel with a diameter of $d = 12.7$ mm were used as counterparts. The steel balls rotated uniformly at a frequency of $f = 1$ Hz, giving a continuous sliding speed of $v = \pi df \cos 45^\circ = 28.2$ mm/s.

The data acquisition was performed via inductive displacement transducers (Fig. 2a). The signals of the displacement transducers were read every 30 min and stored by a PC system.

2.2.2. Creep tests

In technical bearing applications creep as well as wear could cause fitting problems after a long period of loading. In order to separate these two effects as much as possible, special creep tests were performed.

Before starting the wear tests, the specimens were statically loaded in the wear test rig for a duration of about 60 h. Under this static load, the balls penetrated into the specimen surface producing plastic deformation and creep of the specimen surfaces. The loading conditions were the same as described in the testing procedure.

2.2.3. Wear tests

The penetration caused by creep decelerated continuously. After the first 60 h the balls were essentially in rest. When the first 60 h period was completed, the motor of the wear testing apparatus was switched on without unloading the specimens. All tests were performed under dry conditions at room temperature (about 23 °C) and at about 50% RH. At least three specimens were tested of each type of sample material.

2.2.4. Data processing

The signal received from the displacement transducers gave the displacement of the lever in vertical direction, *h*. From these data, the penetration depth of the ball into the specimen surface, *H*, was calculated (Fig. 3) as

$$H = h \sin 45^\circ = \frac{1}{\sqrt{2}} h$$

Fig. 4 shows an example of a typical *H* versus *t* curve. During the first 10 h, the wear proceeds rapidly

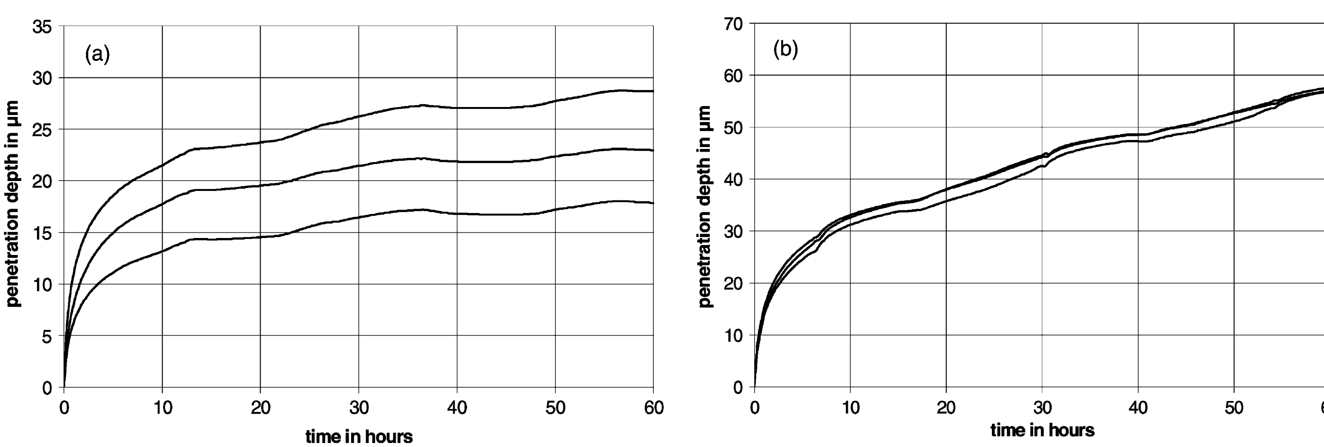

Fig. 5. Typical creep curves. Curve (a) for fibre reinforced 4011 matrix and curve (b) for neat 4041 matrix (highest branching, lowest crystallinity). The wavy fluctuations are due to temperature changes between day and night. The three curves per plot represent three different specimens of the respective material.

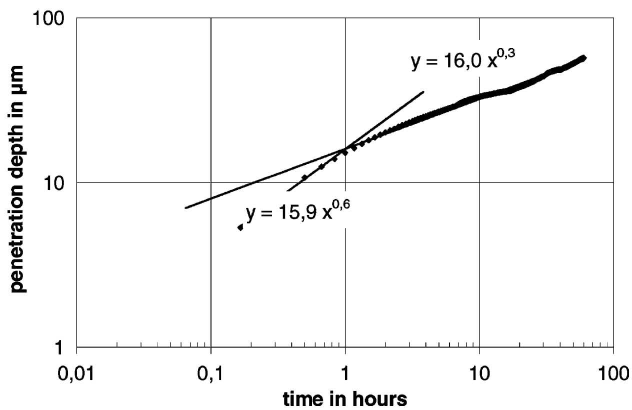

Fig. 6. Log–log plot of the data from Fig. 5b. The potential functions are fitted to the lower and upper part of the experimental curve, respectively.

(running-in-phase), the slope of the H–t curve continuously decreases until it reaches a roughly constant value (steady-state). It was experimentally found that the height–time curve became linear in all cases during the steady-state although the contact area increased continuously. However, the dissipated work does not depend on the contact area but only on the normal load and friction coefficient. A linear function $\Delta H = \Delta H_0 + w_{H/t}\Delta t$ was fitted do the wear data beyond 20 h. The slope of this linear function is the linear wear rate $w_{H/t} = \Delta H/\Delta t$ [16] which was used as a measure for the wear susceptibility of the material during the steady-state. The constant factor ΔH_0 was taken as a quantitative measure for the running-in wear.

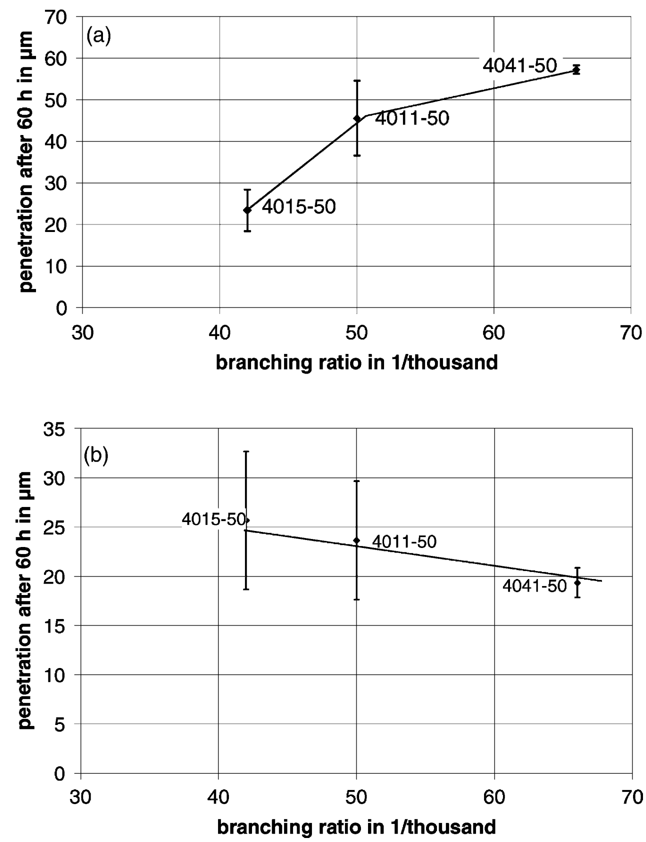

Fig. 8. Correlation between branching ratio and creep susceptibility for the neat matrices (a) and the composites (b). The error bars represent the standard deviation of the data.

3. Results and discussion

3.1. Creep tests

Under static load, the balls penetrate slowly into the polymeric specimens (Fig. 5). This motion decelerates with time for two reasons [14]:

(1) Creep of polymers under constant stresses usually obeys a digressively increasing potential law [17]:

$$\varepsilon = \varepsilon_0 a t^n \Leftrightarrow \log \varepsilon \approx \log a + n \log t, \quad \text{with } n < 1$$

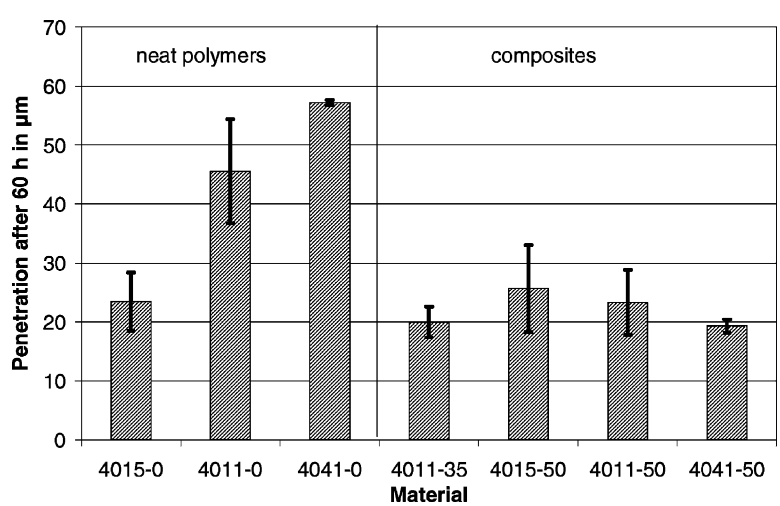

Fig. 7. Compilation of all creep test results. The left three bars represent the neat co-polymer matrices with branching ratio increasing from left to right. The suffix –35 and –50 designates the composites with 35 and 50° winding angle. Error bars represent the standard deviation.

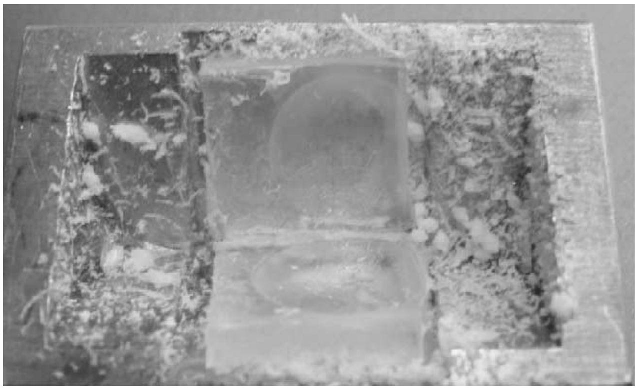

Fig. 9. Photograph of a worn 4011 neat matrix specimen.

If this law would apply, a $\log \varepsilon$ versus $\log t$ plot should give a linear function. However, Fig. 6 shows that this is not true in the case of the balls penetrating into the polymer.

(2) The contact area increases during the penetration process, leading to decreasing contact pressures. For this reason, the exponent of the potential law decreases with time.

For the fibre reinforced versions, creep almost disappears, or more correctly it becomes negligible in comparison to the wear, after about 15 h (Fig. 5a). This is not true for the neat matrices. In these cases the creep rate also decreases very rapidly during the first 15 h but does not approach zero after that time (Fig. 5b).

Fig. 7 summarises the results of creep tests by plotting the penetration depth after 60 h. In all fibre reinforced versions,

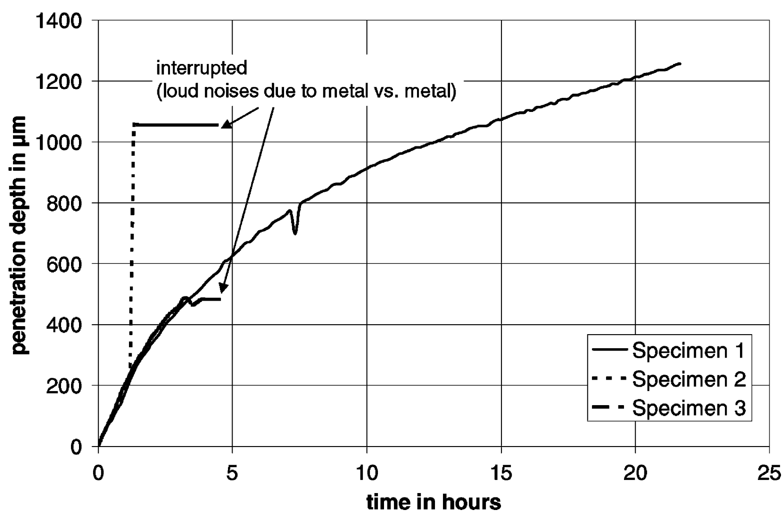

Fig. 10. Wear test on the neat 4011 matrix (for experimental details, see text). One specimen survived 22 h. The other tests were interrupted after a few hours due to load noises caused by metal/metal contact.

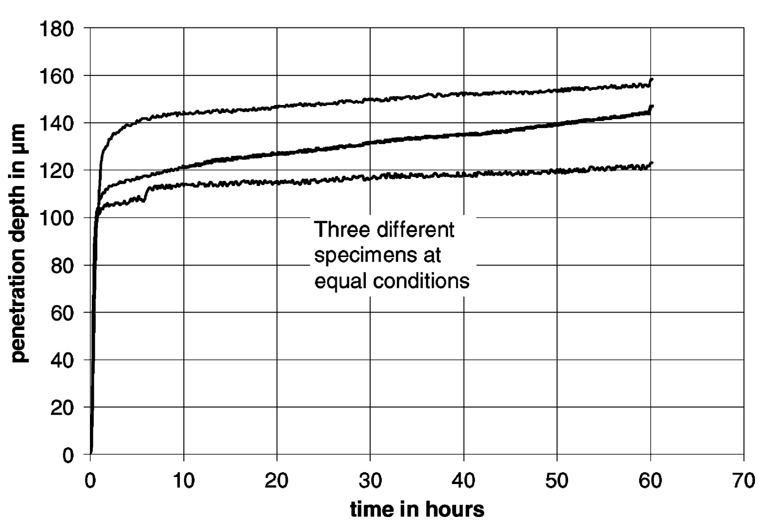

Fig. 11. Wear curves of 4015–50.

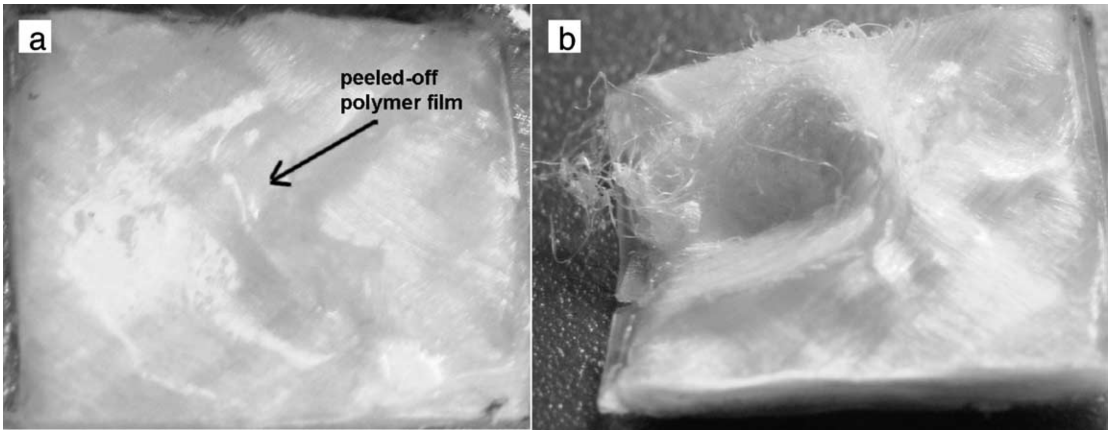

Fig. 12. (a) Photograph of a 4041 composite specimen after 2 min running time. The thin surface layer of neat polymer has already been ruptured and peeled-off. (b) The samples fibrillated more (matrix with high branching) or less (matrix with less branching).

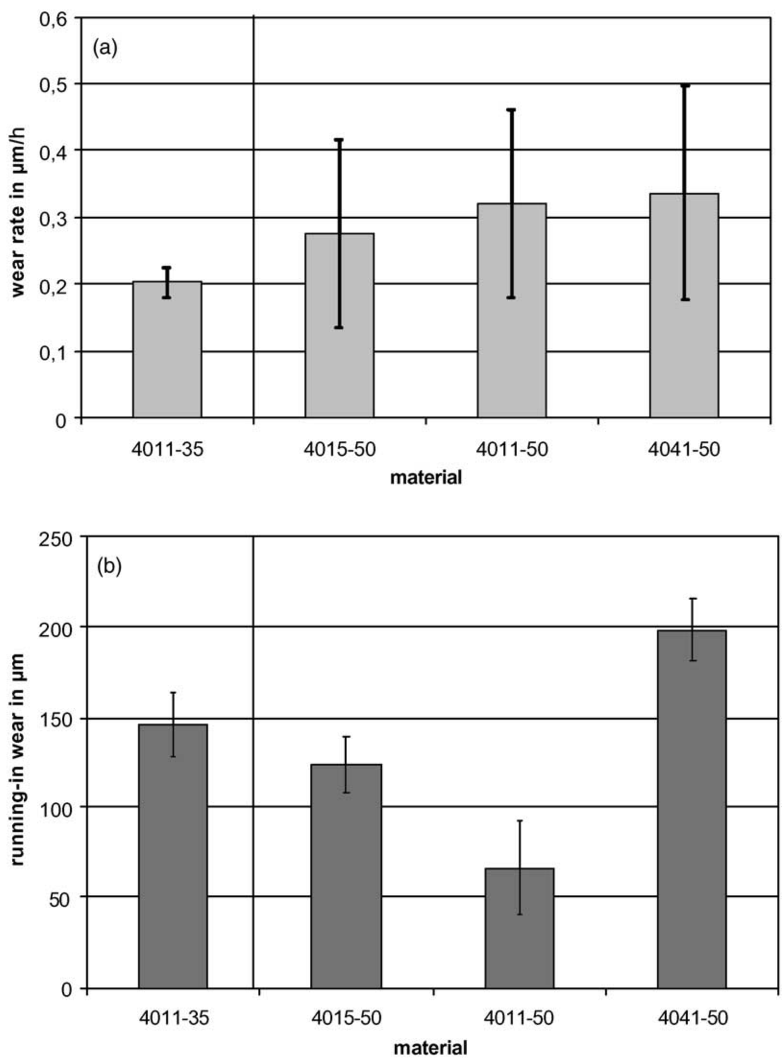

Fig. 13. Compilation of the wear test data of all composite materials tested. (a) Steady-state wear rates and (b) ball penetration depth during the running-in phase. Within the right groups (with the extension –50) the branching ratio increases from left to right.

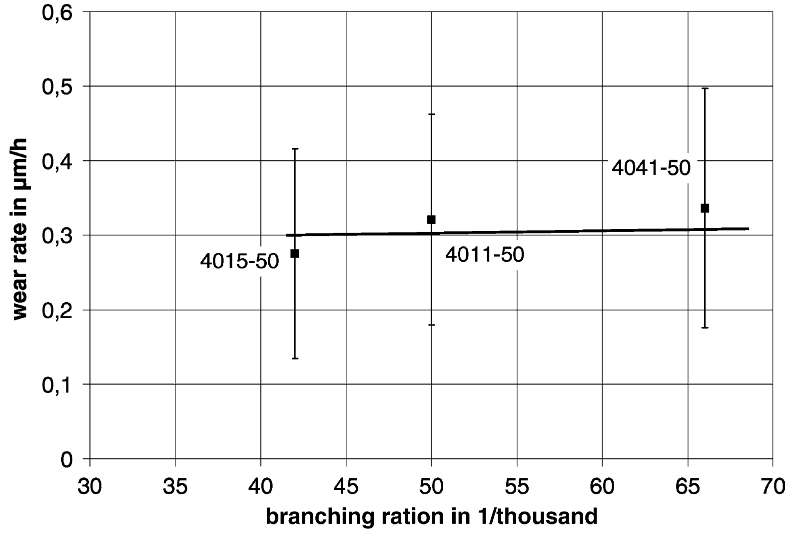

Fig. 14. Correlation of branching ratio and wear rate for the composites with 50° winding angle.

creep was much less than in the neat matrices. For the neat matrices there is a clear trend (Fig. 8a). The creep susceptibility increases with increasing branching ratio (4041 > 4011 > 4015). This is due to decreases in crystallinity and thus the yield stress of the matrix with increasing branching ratio [10].

No correlation between branching ratio of the matrix and composite creep could be found (Fig. 8b), the differences are smaller than the scatter of the data. Also no significant effect of the winding angle was observed. The data of 4011–35 (35° winding angle) and 4011–50 (50° winding angle) in Fig. 7 are essentially the same.

3.2. Wear tests

The neat matrices were rapidly worn (Fig. 9) which is in agreement with the low strength of the rather soft polymers. Most specimens were totally milled within 0.5–3 h. Only one specimen from the 4011 and one from the 4015 grade (the more rigid and less branched polymers) survived 25 h of wear testing with a penetration of 1 mm (Figs. 9 and 10). The even softer matrices of the 4041 type were destroyed almost immediately by being shredded into small pieces instead of being worn steadily. For this reason, no quantitative wear data are reported for the neat matrices.

The wear curves (after a preceding creep phase of 60 h) of the composites exhibited a clearly pronounced running-in phase characterised by a high wear rate and followed by a steady-state phase with a lower and almost constant wear rate dh/dt (Fig. 11). This running-in phase was less distinct or even missing in the wear curves of the neat matrices (Fig. 10). A visual inspection of the wear surfaces gave the explanation of the high running-in wear of the composites (Fig. 12a): the fibres are covered by a thin layer (about 100 µm thick) of the neat matrix. The frictional forces led to rapid rupture and peeling-off of this layer. After this phase, the ball slides over the UHMWPE fibres which have a much higher wear resistance. The steady-state wear rate is therefore relatively low and comparable to earlier measurements on UHMWPE fibres in HD–PE matrix [14]. However, the composites still tend to fibrillate (Fig. 12b) under frictional loading due to relatively weak fibre/matrix bonding.

Fig. 13 summarises the results of the composite wear tests. On the first glimpse it seems that the wear rate again increases with increasing branching ratio. However, Fig. 14 depicts that this effect is small compared with the scatter of the data. The composite wear is masked by the wear behaviour of the fibres. The fibres are distributed somewhat inhomogeneously (see Fig. 1) causing the scatter of the data. The matrix type does not effects the composite wear rate significantly.

The composites with 35° winding angle have a slightly higher wear resistance than the composites with 50°. But this difference again is within the scatter of the experimental data.

The situation is different as far as the running-in wear is concerned (Fig. 13b). The wear data of the composites obviously differ significantly from one to another. However, there is no correlation between branching ratio (4041 > 4011 > 4015) and wear (4041 > 4015 > 4011). Probably, the different running-in wear rates can rather be attributed to production variations than to material properties: the thickness of the neat matrix surface layer which is removed during the running-in phase varies from sample to sample and so does the running-in wear.

4. Conclusions

The simple wear tests presented in this paper were performed as first screening tests to get an impression about the wear behaviour of artificial tendons and ligaments made of UHMWPE fibre reinforced polyethylene–butene copolymers. Specifically, some performance deficiencies became apparent and a few leads for potential improvements could be drawn on the basis of the following conclusions.

- The different properties of the resins (resulting from the different branching densities and degrees of crystallinity) are manifested clearly in the creep results which increase with the branching ratio from around 25–60 μm at 60 h of static penetration. The creep is significantly reduced by the fibre reinforcement.
- The wear results too reflect the properties of the resins, wherein only the more rigid less branched polymers survived 25 h of wear testing with a penetration of more than 1 mm. The softer polymers with higher branching ratio failed almost immediately by rupture.
- The performance of the composites is dominated by the fibres, which mask the properties of the different matrices. There is no significant difference in the values of the steady-state wear rate. The differences in the running-in wear are rather related to random production variations (thickness of the polymeric surface layer) than to intrinsic material properties.
- Neat matrix surface layers are undesirable because of their early destruction by frictional forces. The fibre/matrix bonding of the specimens was insufficient. The specimens were specially produced to fit into the sliding wear apparatus. In order to reach the required thickness, the amount of fibres was increased and the tight packing prevented the resin to wet the fibre tows. Better bonding was observed before in thinner samples [10–12].
- Concerning the effect of the winding angle, it seems that the 35° winding angle provides a higher wear resistance during steady-state than the 50° winding angles. However, due to the large scatter of the results caused by production variations this conclusion is not unequivocal. This especially true for the differences in the running-in wear which is governed by the varying thickness of the surface layer consisting of neat matrix.
- The visual damage documented by photographs of each specimen type confirms the major role of the fibres in controlling the wear behaviour of the composites.

In practical applications, artificial ligaments and tendons experience a combined loading of tensile stresses and rubbing against bones or cartilage in biological environment. Surface damage due to wear reduces the tensile strength of the composite materials [18]. The experiments discussed here, of course, do not completely simulate this situation. However, it can be concluded that the wear performance of the materials tested has to be improved significantly before starting more realistic or even in vivo tests. Especially the fibre matrix bonding and the wear resistance of the surface layer have to be strengthened.

References

[1] J.P. Collier, L.C. Sutula, B.H. Currier, J.H. Currier, R.E. Wooding, I.R. Williams, K.B. Farber, M.B. Mayor, Overview of polyethylene as a bearing material, Clin. Orthop. Relat. Res. 333 (1996) 76–86.

[2] N.P. Suh, M. Mosleh, J. Arinez, Tribology of polyethylene homocomposites, Wear 214 (1998) 231–236.

[3] S. Affatato, B. Bordini, C. Fagnano, P. Taddei, A. Tinti, A. Toni, Effects of the sterilization method on the wear of UHMWPE acetubular cups tested in a hip joint simulator, Biomaterials 23 (2002) 1439–1446.

[4] K. Hirakawa, T.W. Bauer, B.N. Stulberg, A.H. Wilde, Comparison and quantitation of wear debris of failed total hip and total knee arthroplasty, J. Biomed. Mater. Res. 31 (2) (1996) 257–263.

[5] N. Poddevin, M.W. King, R.G. Guidoin, Failure mechanisms of anterior cruciate ligament prostheses: in vitro wear study, J. Biomed. Mater. Res. 38 (4) (1997) 370–381.

[6] D. Dowson, Tribological characteristics of polymers with particular reference to polyethylene, in: D.T. Clark, W.J. Feast (Eds.), Polymer Surfaces, Wiley, Chichester, 1978.

[7] R.M. Rose, W.R. Cimino, Exploratory investigations on the structural dependence of the wear resistance of polyethylene, Wear 77 (1982) 89–104.

[8] L. Dursen, L.E. Claes, A. Ignatius, S. Rubenacker, Comparative animal study of different materials for the replacement of the anterior cruciate ligaments in sheep, in: Proceedings of the Transaction of 20th Annual Meeting of the Society on Biomaterials, Boston, 1994, p. 84.

[9] J.M. Hofste, B.V. Voorn, A.J. Pennings, Mechanical and tribological properties of short discontinuous UHMWPE fiber reinforced UHMWPE, Polym. Bull. 38 (1997) 485–492.

[10] M. Kazanci, D. Cohn, G. Marom, Elastic and viscoelastic behavior of filament wound polyethylene fiber reinforced polyolefin composites, J. Mater. Sci. 36 (2001) 2845–2850.

[11] M. Kazanci, D. Cohn, G. Marom, C. Migliaresi, A. Pegoretti, Fatigue characterization of polyethylene fiber reinforced polyolefin biomedical composites, Composites A 33 (2002) 453–458.

[12] M. Kazanci, D. Cohn, G. Marom, H. Ben-Bassat, Surface oxidation of polyethylene fiber reinforced polyolefin biomedical composites and its effect on cell attachment, J. Mater. Sci.: Mater. Med. 13 (2002) 465–468.

[13] S. Shalom, H. Harel, G. Marom, Fatigue behavior of filament-wound polyethylene composites, Comp. Sci. Tech. 57 (1997) 1423–1427.

[14] O. Jacobs, N. Mentz, A. Poeppel, K. Schulte, Sliding wear performance of HD–PE reinforced by continuous UHMWPE Fibres, Wear 244 (2000) 20–28.

[15] N.N., ISO 7148-2, Beuth Verlag, Berlin, 1999.

[16] N.N., German standard DIN 50323-2: Tribologie-Verschleiß-Teil2: Begriffe, Beuth Verlag, Berlin, 1995.

[17] G.W. Ehrenstein, Mit Kunststoffen konstruieren, Hanser, Munich, 1995.

[18] O. Jacobs, Fretting wear and fretting fatigue of continuous fibre reinforced polymer composites, in: N. Cheremisinoff (Ed.), Handbook of Ceramics and Composites: Mechanical Properties and Speciality Applications, Vol. 2, Marcel Dekker, New York, 1992, pp. 161–213.